Calculation of the local electric field for an infinite array of conducting nanosized objects

2007 J. Phys. A: Math. Theor. 40 853

(http://iopscience.iop.org/1751-8121/40/4/018)

INSTITUTE OF PHYSICS PUBLISHING JOURNAL OF PHYSICS A: MATHEMATICAL AND THEORETICAL

J. Phys. A: Math. Theor. **40** (2007) 853–862 doi:10.1088/1751-8113/40/4/018

Calculation of the local electric field for an infinite array of conducting nanosized objects

Mikyoung Lim[1], Dohyung Kim[2], Sang Youl Kim[3] and Jean-Eric Bourée[2]

[1] Centre de Mathématiques Appliquées, CNRS UMR 7641, Ecole Polytechnique, 91128 Palaiseau, France
[2] Laboratoire de Physique des Interfaces et des Couches Minces, CNRS UMR 7647, Ecole Polytechnique, 91128 Palaiseau, France
[3] Department of Molecular Science and Technology, Ajou University, 443-749 Suwon, Korea

E-mail: jean-eric.bouree@polytechnique.edu

Received 6 June 2006, in final form 7 November 2006
Published 9 January 2007
Online at stacks.iop.org/JPhysA/40/853

Abstract

The electric field for an infinite array of conducting nanosized objects in two-dimensional space has been calculated. The mirror symmetry for this physical problem has been introduced. By taking into account this symmetry, we transform the original problem into an infinite two-dimensional array of nanosized objects with the same solution. The electric field equation of the model has been successfully constructed using a single-layer potential of the periodic Green function. The electric field operator has been introduced. This mathematical approach yields a solution for determining the optimum structure of nanosized electronic devices such as carbon nanotube-based field emitters.

PACS numbers: 02.30.Em, 41.20.Cv

(Some figures in this article are in colour only in the electronic version)

1. Introduction

The electric field on conducting nanosized materials plays a central role for electronic devices. For instance, an array of carbon nanotubes [1] or of silicon carbide [2] are considered as good electron emission sources for the field emission displays and microwave cold cathodes. The goal of the field emission study on nanostructured materials is to obtain the highest current density at a low applied electric field. The most dominant factor to achieve this aim, as also revealed in experimental studies [3–9], is the magnitude of the local electric field at an emitter.

Since the individual emitter consisting of one carbon nanotube has been realized [1], it is getting more important to investigate the local electric field on the tip of an individual nanomaterial array. In order to obtain high local electric fields, an array of emitters with a high aspect ratio (long length l divided by short tip radius of curvature r) is required. The

current density can be calculated by using the Fowler–Nordheim equation [10, 11] when the local electric field on the emission tip is determined [12–15].

The electric field calculation of a one-dimensional or a two-dimensional array of nanosized objects should be approached by different ways in comparison with the conventional method (finite difference or finite element method), because it is difficult to obtain the exact value of electric field on such a structure due to its size effect like high aspect ratio ($l/r > 100$). For instance, in the case of multi-walled carbon nanotubes, several studies [12–15] by using a conventional method describe essentially its tendency without giving any exact value. Furthermore, most calculation methods rely on a great computing power.

Recently, Kokkorakis *et al* calculated the local electric field of the open and closed carbon nanotubes [16, 17], but they assumed the shape of cathode to be spherical. Buldum and Lu calculated the effective potential of electrons of carbon nanotubes using a self-consistent field-pseudopotential electronic structure calculation method [18]. However the cathode—anode distance has been assumed as infinite in this calculation and it is difficult to calculate the field of an array of electron emitters. Wang *et al* found analytic solutions of the local electric field for the floating sphere model [19, 20]. It was based on an analytically improved model, but it had intrinsic limits for describing the potential of a nanotube due to the assumption that the tip of a nanotube is in floating position from the cathode. Oh *et al* investigated the field emission properties of carbon nanotube paste layer [21], but it was not an array structure of single-standing nanosized objects.

There are mathematical approaches for solving electric field of biological materials [22, 23] and nanoscale materials [24]. Their studies give a prospective way for solving our physical model. In the present study, the mirror symmetry of local electric field on the boundary of single-standing and nanosized objects arranging in a row in two-dimensional space has been constructed. And then the electric field operator has been introduced. Finally the strength of local electric field on the exact boundary of the infinite array of nanosized objects is calculated using a single-layer potential of the periodic Green function. Our result can be applied to any shape of linear arrays. For applications, we focus on an array of nanotube-shaped objects in two-dimensional space. Last, the emission current density issued from an infinite array of nanosized objects has been investigated.

2. Boundary conditions

The original physical problem and transformation of a boundary condition applied to a unit cell with mirror symmetry into a two-dimensional array of nanosized objects is shown in figure 1. Nanosized objects constitute a rectangular body and a hemispherical solid on the body. Their dimensions for physical applications will be mentioned in section 4. They are assumed to be perfect conductors. In order to eliminate mathematically critical points, mirror symmetry with a basis of potential 0 V line is employed to the system, i.e., the electric potential u is extended such that it is a potential in $\mathbb{R} \times (-m_2/2, m_2/2)$ by defining $u(x, -y) = -u(x, y)$, and then we take again mirror symmetry with a basis of potential $\pm\Phi_0$. This problem is mathematically easier to approach than the original one. Since we take the 0 level line $y = 0$ as the reflection axis, u is smooth across it and satisfies

$$\begin{cases} \nabla^2 u(\mathbf{x}) = 0, & \text{for} \quad \mathbf{x} \in Y \backslash \bar{D}, \\ u(\mathbf{x}) = 0, & \text{for} \quad \mathbf{x} \in \bar{D}. \end{cases} \tag{1}$$

Now let us define a linear function Φ by $\Phi(x, y) = E_{\text{ext}} \times y$ with the external electric field $E_{\text{ext}} (= \Phi_0/(m_2/2))$. Note that on the two boundary lines $y = m_2/2$ and

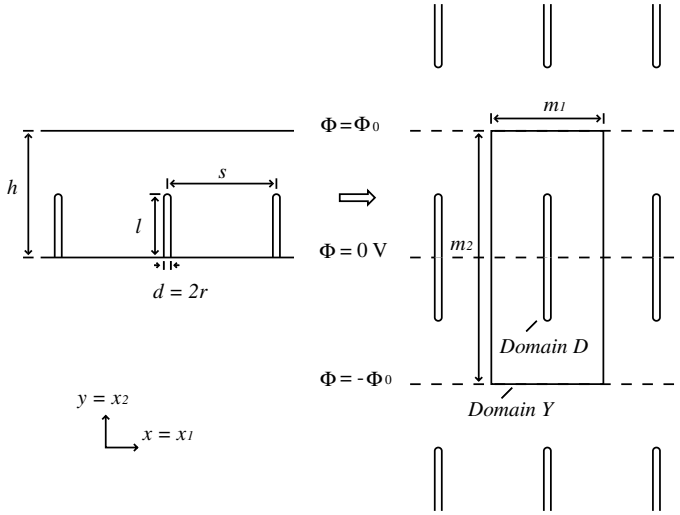

Figure 1. Original physical problem and transformation of a boundary condition applied to a unit cell with mirror symmetry into a two-dimensional array of nanosized objects.

$y = -m_2/2$, $(u - \Phi_0)$ is constantly 0 and has the same gradient. With the x-periodicity due to the arrangement of nanotubes, we can write

$$(u - \Phi_0) \text{ is periodic in } x \text{ and } y \tag{2}$$

with the reference cell $Y = (-m_1/2, m_1/2) \times (-m_2/2, m_2/2)$.

3. Derivation of the local electric field

We start deriving a key formula for the local electric field $E\,(= \partial u/\partial n')$ by using Green formulae of u for $\mathbf{x} \in Y \backslash \bar{D}$:

$$\begin{aligned} u(\mathbf{x}) &= \oint_{\partial Y} \frac{\partial \Gamma}{\partial n'}(\mathbf{x} - \mathbf{x}')u(\mathbf{x}')\,\mathrm{d}\mathbf{x}' - \oint_{\partial Y} \Gamma(\mathbf{x} - \mathbf{x}')\frac{\partial u}{\partial n'}(\mathbf{x}')\,\mathrm{d}\mathbf{x}' \\ &\quad - \oint_{\partial D} \frac{\partial \Gamma}{\partial n'}(\mathbf{x} - \mathbf{x}')u(\mathbf{x}')\,\mathrm{d}\mathbf{x}' + \oint_{\partial D} \Gamma(\mathbf{x} - \mathbf{x}')\frac{\partial u}{\partial n'}(\mathbf{x}')\,\mathrm{d}\mathbf{x}' \\ &= A_1 + A_2 + A_3 + A_4, \end{aligned} \tag{3}$$

where n' is the outward unit normal vector on the boundary point $\mathbf{x}'$, $\partial u/\partial n'$ is defined as $\nabla u \cdot n'$, and $\Gamma(\mathbf{x})(:= 1/2\pi \times \ln|\mathbf{x}|)$ is the fundamental solution of the Laplacian ∇^2 in $\mathbb{R}^2$. A compact expression of $u(x)$ only with $\partial u(\mathbf{x}')/\partial n'$, and $\mathbf{x}' \in \partial D$ can be obtained as follows. Firstly, $A_3 = 0$ since u is constantly 0 on ∂D, secondly, we replace Γ by a periodic Green function G, which satisfies

$$\begin{cases} \nabla^2 G(\mathbf{x} - \mathbf{x}') = \delta(\mathbf{x} - \mathbf{x}') - \dfrac{1}{m_1 m_2} & \text{in } Y \\ G \text{ is periodic w.r.t. } Y. \end{cases} \tag{4}$$

Note that a constant difference between $\nabla^2 G(\mathbf{x} - \mathbf{x}')$ and $\delta(\mathbf{x} - \mathbf{x}')$ in equation (4) has no effect on equation (3) due to $\int_{Y \backslash \bar{D}} u(\mathbf{x}')\,\mathrm{d}\mathbf{x}' = 0$. The periodicity of G, $(u - \Phi)$ and $\nabla\Phi$

implies that the values of $G(\mathbf{x}-\mathbf{x}')\nabla u(\mathbf{x}')$ at two opposite points $\mathbf{x}'$'s on ∂Y are the same, while those of n' have the opposite direction, hence we have $A_2 = 0$.

Now replacing $u(\mathbf{x}')$ by $\Phi(\mathbf{x}')$ and applying Green formulae to Φ, A_1 is identified to be $\Phi(\mathbf{x}')$:

$$\begin{aligned} A_1 &= \oint_{\partial Y} \frac{\partial G}{\partial n'}(\mathbf{x}-\mathbf{x}')\Phi(\mathbf{x}')\,\mathrm{d}\mathbf{x}' \\ &= \oint_{\partial Y} \frac{\partial G}{\partial n'}(\mathbf{x}-\mathbf{x}')\Phi(\mathbf{x}')\,\mathrm{d}\mathbf{x}' - \oint_{\partial Y} G(\mathbf{x}-\mathbf{x}')\frac{\partial \Phi}{\partial n'}(\mathbf{x}')\,\mathrm{d}\mathbf{x}' \\ &= \Phi(\mathbf{x}). \end{aligned}$$

Here the periodicity of $(u-\Phi)$, G and $\nabla\Phi$ are used again.

In conclusion, we have

$$u(\mathbf{x}) = \Phi(\mathbf{x}) + \oint_{\partial D} G(\mathbf{x}-\mathbf{x}')E(\mathbf{x}')\,\mathrm{d}\mathbf{x}', \qquad \text{for} \qquad \mathbf{x} \in Y\backslash\bar{D}, \tag{5}$$

where $E = \partial u/\partial n'$ is the local electric field. Moreover, since the right-hand side of equation (5) is harmonic inside D and 0 on ∂D from equation (1), we have

$$0 = \Phi(\mathbf{x}) + \oint_{\partial D} G(\mathbf{x}-\mathbf{x}')E(\mathbf{x}')\,\mathrm{d}\mathbf{x}', \qquad \text{for} \qquad \mathbf{x} \in D. \tag{6}$$

Differentiating equation (6), the following formula is obtained [25]:

$$E = \left(\frac{1}{2}I - \mathcal{K}_D^*\right)^{-1}\left(\frac{\partial \Phi}{\partial n}\right), \tag{7}$$

where $\mathcal{K}_D^*$ is defined by

$$\mathcal{K}_D^* E(\mathbf{x}) = \text{p.v.} \int_{\partial D} \frac{\partial}{\partial n} G(\mathbf{x}-\mathbf{x}')E(\mathbf{x}')\,\mathrm{d}\mathbf{x}'. \tag{8}$$

The electric field operator has been defined by the inverse of $(I/2-\mathcal{K}_D^*)$. The invertability of the operator $(I/2-\mathcal{K}_D^*)$ on $L_0^2(\partial D) = \{f \in L^2(\partial D) : \int_{\partial D} f\,\mathrm{d}\mathbf{x} = 0\}$ is verified and a representation of the periodic Green function G is obtained [25].

$$G(\mathbf{x}) = -\frac{1}{m_1 m_2} \sum_{n \in \mathbb{Z}^2\backslash\{0\}} \frac{\exp\left(\mathrm{i}2\pi n \cdot \left(\frac{x_1}{m_1}, \frac{x_2}{m_2}\right)\right)}{4\pi^2\left(\frac{n_1^2}{m_1^2} + \frac{n_2^2}{m_2^2}\right)}. \tag{9}$$

Then we get

$$\begin{aligned} \nabla^2 G(\mathbf{x}) &= \frac{1}{m_1 m_2} \sum_{n \in \mathbb{Z}^2\backslash\{0\}} \exp\left(\mathrm{i}2\pi n \cdot \left(\frac{x_1}{m_1}, \frac{x_2}{m_2}\right)\right) \\ &= \frac{1}{m_1 m_2} \sum_{n \in \mathbb{Z}^2} \exp\left(\mathrm{i}2\pi n \cdot \left(\frac{x_1}{m_1}, \frac{x_2}{m_2}\right)\right) - \frac{1}{m_1 m_2}, \end{aligned} \tag{10}$$

and from the Poisson summation formulae,

$$\begin{aligned} \sum_{n \in \mathbb{Z}^2} \exp\left(\mathrm{i}2\pi n \cdot \left(\frac{x_1}{m_1}, \frac{x_2}{m_2}\right)\right) &= \sum_{n \in \mathbb{Z}^2} \delta\left(\left(\frac{x_1}{m_1}, \frac{x_2}{m_2}\right) + n\right) \\ &= m_1 m_2 \sum_{n \in \mathbb{Z}^2} \delta(x + (m_1 n_1, m_2 n_2)). \end{aligned} \tag{11}$$

With equations (10) and (11), it turns out that G, defined as equation (9), satisfies equation (4). Using summation identities, the convergence of equation (9) can be proved. Recall the mirror

symmetry with a basis of potential 0 V (see figure 1) and equation (9) in order to represent (see [25])

$$\begin{aligned} m_1 m_2 G(x) &= -\sum_{n\in\mathcal{Z}^2\setminus\{0\}} \frac{\exp\left(\mathrm{i}2\pi n\cdot\left(\frac{x_1}{m_1},\frac{x_2}{m_2}\right)\right)}{4\pi^2\left(\frac{n_1^2}{m_1^2}+\frac{n_2^2}{m_2^2}\right)} \\ &= -\frac{1}{4\pi^2}\sum_{n\in\mathcal{Z}^2\setminus\{0\}} \frac{\cos 2\pi n_1\frac{x_1}{m_1}\cos 2\pi n_2\frac{x_2}{m_2}}{\frac{n_1^2}{m_1^2}+\frac{n_2^2}{m_2^2}} \\ &= -\frac{1}{2\pi^2}\sum_{n_1=0}^{+\infty}\cos 2\pi n_1\frac{x_1}{m_1}\sum_{n_2=1}^{+\infty}\frac{\cos 2\pi n_2\frac{x_2}{m_2}}{\frac{n_1^2}{m_1^2}+\frac{n_2^2}{m_2^2}} \\ &\quad -\frac{1}{2\pi^2}\sum_{n_2=0}^{+\infty}\cos\left(2\pi n_2\frac{x_2}{m_2}\right)\sum_{n_1=1}^{+\infty}\frac{\cos 2\pi n_1\frac{x_1}{m_1}}{\frac{n_1^2}{m_1^2}+\frac{n_2^2}{m_2^2}} \\ &= G_1+G_2. \end{aligned} \tag{12}$$

Let us invoke three summation identities (see for instance [26]):

$$\sum_{n_2=1}^{+\infty}\frac{\cos 2\pi n_2\frac{x_2}{m_2}}{\frac{n_1^2}{m_1^2}+\frac{n_2^2}{m_2^2}} = m_2^2\sum_{n_2=1}^{+\infty}\frac{\cos 2\pi n_2\frac{x_2}{m_2}}{\frac{m_2^2}{m_1^2}n_1^2+n_2^2}$$

$$= \begin{cases} -\dfrac{m_1^2}{2n_1^2}+\dfrac{m_1m_2\pi}{2n_1}\dfrac{\cosh\pi(2x_2-m_2)\frac{n_1}{m_1}}{\sinh\pi\frac{m_2}{m_1}n_1} & \text{if} \quad n_1\neq 0, \\ \dfrac{m_2^2\pi^2}{6}-m_2\pi^2x_2+\pi^2x_2^2 & \text{if} \quad n_1=0. \end{cases}$$

$$\sum_{n_1=1}^{+\infty}\frac{\cos 2\pi n_1\frac{x_1}{m_1}}{n_1}\exp\left(-2\pi n_1\frac{x_2}{m_1}\right) = \pi\frac{x_2}{m_1}-\log 2-\frac{1}{2}\log\left(\sinh^2\pi\frac{x_2}{m_1}+\sin^2\pi\frac{x_1}{m_1}\right).$$

We then compute

$$\begin{aligned} G_1 &= -\frac{m_2^2}{2\pi^2}\sum_{n_2=1}^{+\infty}\frac{\cos 2\pi n_2\frac{x_2}{m_2}}{n_2^2} \\ &\quad -\frac{1}{2\pi^2}\sum_{n_1=1}^{+\infty}\cos\left(2\pi n_1\frac{x_1}{m_1}\right)\left[-\frac{m_1^2}{2n_1^2}+\frac{m_1m_2\pi}{2n_1}\frac{\cosh\pi(2x_2-m_2)\frac{n_1}{m_1}}{\sinh\pi\frac{m_2}{m_1}n_1}\right] \\ &= -\frac{m_2^2}{2\pi^2}\sum_{n_2=1}^{+\infty}\frac{\cos 2\pi n_2\frac{x_2}{m_2}}{n_2^2}+\frac{m_1^2}{4\pi^2}\sum_{n_1=1}^{+\infty}\frac{\cos\left(2\pi n_1\frac{x_1}{m_1}\right)}{n_1^2} \\ &\quad -\frac{m_1m_2}{4\pi}\sum_{n_1=1}^{+\infty}\frac{\cos\left(2\pi n_1\frac{x_1}{m_1}\right)}{n_1}\frac{\cosh\pi(2x_2-m_2)\frac{n_1}{m_1}}{\sinh\pi\frac{m_2}{m_1}n_1} \\ &= -\frac{m_2^2}{12}+\frac{m_2}{2}x_2-\frac{1}{2}x_2^2+\frac{m_1^2}{24}-\frac{m_1}{4}x_1+\frac{1}{4}x_1^2 \\ &\quad -\frac{m_1m_2}{4\pi}\sum_{n_1=1}^{+\infty}\frac{\cos\left(2\pi n_1\frac{x_1}{m_1}\right)}{n_1}\mathrm{e}^{-2\pi\frac{n_1}{m_1}x_2} \\ &\quad -\frac{m_1m_2}{4\pi}\sum_{n_1=1}^{+\infty}\frac{\cos\left(2\pi n_1\frac{x_1}{m_1}\right)}{n_1}\left[\frac{\cosh\pi(2x_2-m_2)\frac{n_1}{m_1}}{\sinh\pi\frac{m_2}{m_1}n_1}-\mathrm{e}^{-2\pi\frac{n_1}{m_1}x_2}\right] \end{aligned}$$

to arrive at

$$G_1 = -\frac{2m_2^2 - m_1^2}{24} + \frac{m_1 m_2 \log 2}{4\pi} - \frac{1}{4}(m_1 x_1 - m_2 x_2) - \frac{1}{4}\left(2x_2^2 - x_1^2\right) + \frac{m_1 m_2}{8\pi} \log\left(\sinh^2 \pi \frac{x_2}{m_1} + \sin^2 \pi \frac{x_1}{m_1}\right) + r_1(x), \tag{13}$$

where the function $r_1(x)$ is given by

$$r_1(x) = -\frac{m_1 m_2}{4\pi} \sum_{n_1=1}^{+\infty} \frac{\cos\left(2\pi n_1 \frac{x_1}{m_1}\right)}{n_1} \left[\frac{\cosh \pi (2x_2 - m_2)\frac{n_1}{m_1}}{\sinh \pi \frac{m_2}{m_1} n_1} - \mathrm{e}^{-2\pi \frac{n_1}{m_1} x_2}\right]$$
$$= -\frac{m_1 m_2}{4\pi} \sum_{n_1=1}^{+\infty} \frac{\cos\left(2\pi n_1 \frac{x_1}{m_1}\right)}{n_1} \frac{\mathrm{e}^{2\pi n_1 \frac{x_2}{m_1}} + \mathrm{e}^{-2\pi n_1 \frac{x_2}{m_1}}}{\mathrm{e}^{2\pi \frac{m_2}{m_1} n_1} - 1}.$$

In the same way,

$$G_2 = -\frac{2m_1^2 - m_2^2}{24} + \frac{m_1 m_2 \log 2}{4\pi} + \frac{1}{4}(m_1 x_1 - m_2 x_2) - \frac{1}{4}\left(2x_1^2 - x_2^2\right) + \frac{m_1 m_2}{8\pi} \log\left(\sinh^2 \pi \frac{x_1}{m_2} + \sin^2 \pi \frac{x_2}{m_2}\right) + r_2(x), \tag{14}$$

where the function $r_2(x)$ is given by

$$r_2(x) = -\frac{m_1 m_2}{4\pi} \sum_{n_2=1}^{+\infty} \frac{\cos\left(2\pi n_2 \frac{x_2}{m_2}\right)}{n_2} \left[\frac{\cosh \pi (2x_1 - m_1)\frac{n_2}{m_2}}{\sinh \pi \frac{m_2}{m_1} n_2} - \mathrm{e}^{-2\pi \frac{n_2}{m_2} x_1}\right]$$
$$= -\frac{m_1 m_2}{4\pi} \sum_{n_2=1}^{+\infty} \frac{\cos\left(2\pi n_2 \frac{x_2}{m_2}\right)}{n_2} \frac{\mathrm{e}^{2\pi n_2 \frac{x_1}{m_2}} + \mathrm{e}^{-2\pi n_2 \frac{x_1}{m_2}}}{\mathrm{e}^{2\pi \frac{m_1}{m_2} n_2} - 1}.$$

In conclusion,

$$m_1 m_2 G(\mathbf{x}) = C - \frac{x_1^2 + x_2^2}{4} + r_1(x) + r_2(x) + \frac{m_1 m_2}{8\pi} \log\left(\sinh^2 \frac{\pi x_2}{m_1} + \sin^2 \frac{\pi x_1}{m_1}\right) + \frac{m_1 m_2}{8\pi} \log\left(\sinh^2 \frac{\pi x_1}{m_2} + \sin^2 \frac{\pi x_2}{m_2}\right), \tag{15}$$

where C is a constant and

$$r_1(x) = -\frac{m_1 m_2}{4\pi} \sum_{n_1=1}^{+\infty} \frac{\cos\left(2\pi n_1 \frac{x_1}{m_1}\right)}{n_1} \frac{\mathrm{e}^{2\pi n_1 \frac{x_2}{m_1}} + \mathrm{e}^{-2\pi n_1 \frac{x_2}{m_1}}}{\mathrm{e}^{2\pi \frac{m_2}{m_1} n_1} - 1}, \tag{16}$$

$$r_2(x) = -\frac{m_1 m_2}{4\pi} \sum_{n_2=1}^{+\infty} \frac{\cos\left(2\pi n_2 \frac{x_2}{m_2}\right)}{n_2} \frac{\mathrm{e}^{2\pi n_2 \frac{x_1}{m_2}} + \mathrm{e}^{-2\pi n_2 \frac{x_1}{m_2}}}{\mathrm{e}^{2\pi \frac{m_1}{m_2} n_2} - 1}. \tag{17}$$

Now we can compute equation (7), and we get the local electric field strength on the surface of a nanosized object such as a carbon nanotube. The example of the solution for carbon nanotubes array is introduced in the following section. Henceforth we shall define the field enhancement factor γ as the ratio of the local electric field to the external electric field

$$E_{\mathrm{ext}} = \Phi_0/(m_2/2), \tag{18}$$

$$\gamma \equiv E/E_{\mathrm{ext}}. \tag{19}$$

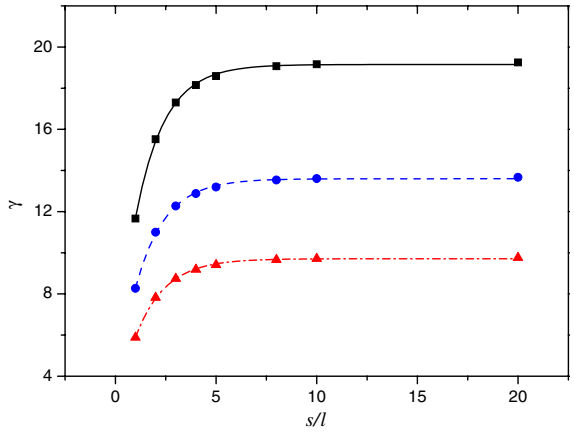

Figure 2. The spacing dependence of the field enhancement factor γ for different nanotube diameters, $d = 10$ nm (square), 20 nm (circle) and 40 nm (triangle), as a function of spacing between nanotubes.

4. Computation results

For applications, we focus on an infinite array of nanotube-shaped objects (domain D in figure 1) in two-dimensional space. The screening effect comes from the repulsive interaction between neighbouring conducting nanotubes spaced s ($= m_1$ in figure 1) apart. The dependence of γ for different aspect ratios as a function of spacing between nanotubes s (as referred to the nanotube length l) is shown in figure 2. The nanotubes are 1 μm in length and 10 nm, 20 nm and 40 nm in diameter d ($l/r = 200$, 100 and 50). In all cases the field enhancement factors γ saturate when s is about 8 times as large as l, which corresponds to a nanotube density of about 10^6 nanotubes cm^{-2}. In other words, as the spacing between nanotubes decreases, γ decreases due to the increasing screening effect.

The normalized field enhancement factors of figure 2 reach a consensus: as long as $d < s/10$, the diameter of nanotubes does not affect the screening effect within our computation tolerance. When the nanotubes become more dense, the diameter effect is appearing. The function of the screening effect can be extracted from the calculations (lines in figure 2).

$$\gamma(s/l) = \gamma(s_\infty)[1 - p \cdot \exp(-q \cdot s/l)], \tag{20}$$

where $\gamma(s/l)$ is a field enhancement factor and $\gamma(s_\infty)$ is that of a free-standing case without neighbouring nanotubes. The p and q are screening constants. In this case, p is 0.76, and q is 0.66. The introduction of p gives a better accuracy to describe the screening effect.

For the detailed investigation of the field enhancement factor, let us consider the variation of γ versus the position along the tip of a nanotube (figure 3). θ is polar coordinate referred to the centre of the semicircle shaped tip on the vertical line through the apex as origin (see small box in figure 3). A nanotube is 10 μm in length and 10 nm in diameter. γ significantly decreases with opening θ. According to the Fowler–Nordheim equation that governs the field emission, the current density exponentially increases with increase of the electric field. It means that the specific region near the apex contributes to the total current.

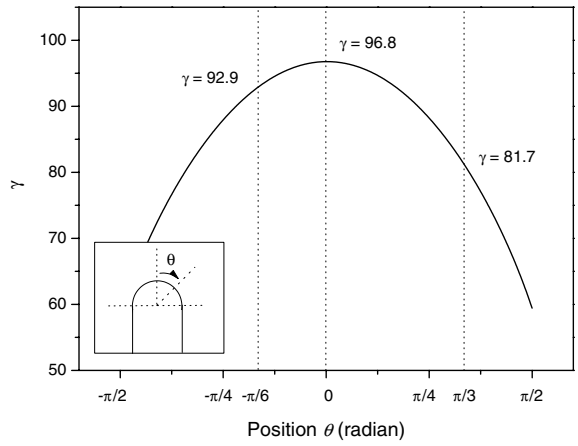

Figure 3. The field enhancement factor along the semicircle shaped tip as a function of the position in radian. θ is polar coordinate referred to the centre of the semicircle shaped tip on the vertical line through the apex as origin (insert).

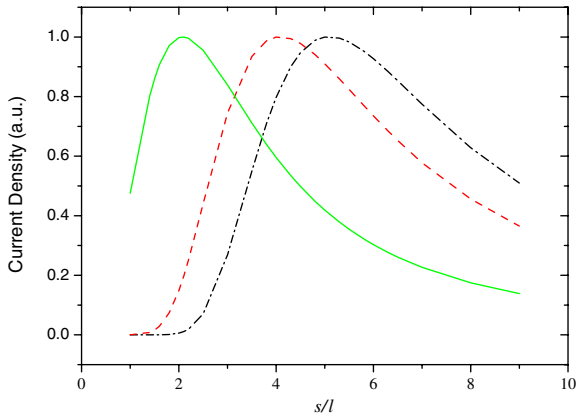

Figure 4. Normalized current densities for different initial local electric fields. The initial local electric field is chosen as 1.5 (dash-dotted line), 3.0 (dashed line) and 15.0 (solid line) kV μm^{-1}.

The current density is calculated by the Fowler–Nordheim equation as follows [10, 11]:

$$J = \frac{AF^2}{\phi t^2(y)} \exp\left[\frac{-Bv(y)\phi^{3/2}}{F}\right], \tag{21}$$

where F is the local electric field at the tip in V/cm, ϕ is the work function of the nanotube emitter in eV, $t^2(y)$ and $v(y)$ are electric field-dependent elliptical functions and y is the image charge lowering contribution to the work function. A and B are the Fowler–Nordheim constants given by 1.54×10^{-3} and 6.87×10^7. Given these definitions, the electric field-dependent elliptical functions can be written $t^2(y) = 1.1$, $v(y) = 0.95 - y^2$ and $y = 3.79 \times 10^{-4} F^{1/2}/\phi$ [27]. The work function of a multi-wall carbon nanotube emitter is set to be 5 eV in this study [28, 29]. The current density J is in mA cm^{-2}.

When the spacing between nanotubes is small, the magnitude of the local electric field decreases due to the screening effect from neighbouring nanotubes. When the spacing is

large, the current density decreases steadily due to the decreasing number of emission sources in a unit surface. Taking into account these opposite trends, an optimization of the total current density can be obtained. For clearness of the relation between the current density and spacing, we examine the normalized current densities for different initial local electric fields F_0 (figure 4). F_0 is the local electric field for a single nanotube in free space. In figure 4, F_0 is chosen as 1.5 , 3.0 and 15.0 kV μm^{-1}. The spacing s is expressed as referred to the nanotube length l. As we discussed, the local electric field decreases with the decrease of spacing (or s/l). Several researchers pointed that the optimum spacing is twice as large as the length of a nanotube [12, 13, 28]. This is partially true. As can be observed in figure 4, higher and higher local electric fields induce a shift of the current density maximum towards lower values of spacing (or of s/l). For instance, when F_0 is chosen as 1.5 kV μm^{-1}, the maximum current density is found for $s = 5l$; when F_0 is chosen as 15 kV μm^{-1}, the maximum is found for $s = 2l$. This trend can be explained, taking into account the experimental dependence of the current density as a function of the local electric field (equation (21)).

5. Conclusion

The local electric field problem concerning an infinite array of nanosized objects has been solved. By taking into account the mirror symmetry, the linear array problem has been transformed into a two-dimensional array problem, which is mathematically easier to handle. The periodic Green function has been expanded, and then the electric field operator has been successfully deduced using the boundary layer technique.

Using the mathematical approach, the value of the local electric field associated with an array of nanotube tips has been estimated as well as the value of the current density for a given nanotube length as a function of the nanotube spacing. From this work, a trend giving local values of nanotube spacing has been deduced from the model when the local electric field acting on the nanotube tips increases. Thus an optimum of the emission current density has been found for a linear assembly of conducting nanosized objects.

Acknowledgments

This work is supported by CNRS-KOSEF international joint research project (KOSEF No. F01-2004-000-10240-0). Dr Lim is partially supported by the post-doctoral fellowship program of the Korea Science and Engineering Foundation.

References

[1] Teo K B K, Minoux E, Hudanski L, Peauger F, Schnell J-P, Gangloff L, Legagneux P, Dieumegard D, Amaratunga G A J and Milne W I 2005 *Nature* **437** 968
[2] Lo H C, Das D, Hwang J S, Chen K H, Hsu C H, Chen C F and Chen L C 2003 *Appl. Phys. Lett.* **83** 1420
[3] Collins P G and Zettl A 1997 *Phys. Rev.* B **55** 9391
[4] Chhowalla M, Ducati C, Rupesinghe N L, Teo K B K and Amaratunga G A J 2001 *Appl. Phys. Lett.* **79** 2079
[5] Bonard J-M, Dean K A, Coll B F and Klinke C 2002 *Phys. Rev. Lett.* **89** 197602
[6] Suh J S, Jeong K S, Lee J S and Han I 2002 *Appl. Phys. Lett.* **80** 2392
[7] Bonard J-M, Croci M, Klinke C, Conus F, Arfaoui I, Stöckli T and Chatelain A 2003 *Phys. Rev.* B **67** 085412
[8] Bonard J-M, Klinke C, Dean K A and Coll B F 2003 *Phys. Rev.* B **67** 115406
[9] Jo S H, Tu Y, Huang Z P, Carnahan D L, Wang D Z and Ren Z F 2003 *Appl. Phys. Lett.* **82** 3520
[10] Fowler R H and Nordheim L 1928 *Proc. R. Soc.* A **119** 173
[11] Nordheim L W 1928 *Proc. R. Soc. Lond.* **121** 626
[12] Nilsson L, Groening O, Kuettel O, Schaller E, Schlapbach L, Kind H, Bonard J-M and Kern K 2000 *Appl. Phys. Lett.* **76** 2071

[13] Bonard J-M, Weiss N, Kind H, Stöckli T, Forró L, Kern K and Châtelain A 2001 *Adv. Mater.* **13** 184
[14] Edgcombe C J and Valdrè U 2001 *J. Micros.* **203** 188
[15] Kim D, Bourée J-E and Kim S Y 2006 *Appl. Phys.* A **83** 111
[16] Kokkorakis C G, Modinos A and Xanthakis J P 2002 *J. Appl. Phys.* **91** 4580
[17] Kokkorakis C G, Roumeliotis J A and Xanthakis J P 2004 *J. Appl. Phys.* **95** 1468
[18] Buldum A and Lu J P 2003 *Phys. Rev. Lett.* **91** 236801
[19] Wang X Q, Wang M, He P M, Xu Y B and Li Z H 2004 *J. Appl. Phys.* **96** 6752
[20] Wang M, Li Z H, Shang X F, Wang X Q and Xu Y B 2005 *J. Appl. Phys.* **98** 014315
[21] Oh T S, Yoo J B, Park C Y, Lee S E, Lee J H and Kim J M 2005 *J. Appl. Phys.* **98** 084313
[22] Ouroushev D 1998 *J. Phys. A: Math. Gen.* **31** 3897
[23] Irimia A 2005 *J. Phys. A: Math. Gen.* **38** 8123
[24] Scott R, Boland M, Rogale K and Fernǎndez A 2004 *J. Phys. A: Math. Gen.* **37** 9791
[25] Ammari H, Kang H and Touibi K 2005 *Asymptotic Anal.* **41** 119
[26] Collin R E 1991 *Field Theory of Guided Waves* 2nd edn (New York: IEEE) p 813
[27] Spindt C A, Brodie I, Humphrey L and Westerberg E R 1976 *J. Appl. Phys.* **47** 5248
[28] Gröning O, Kuttel O M, Emmenegger C, Groning P and Schlapbach L 2000 *J. Vac. Sci. Technol.* B **18** 665
[29] Bonard J-M, Croci M, Arfaoui I, Noury O, Sarangi D and Chatelain A 2002 *Diam. Relat. Mater.* **11** 763